ISSN 2963-7511
Journal of Engineering Researcher and Lecturer, Vol. 3, No. 3, pp. 137-158, 2024

Removal of lead and cadmium from aqueous solution by using cashew gum polysaccharide (Arabinogalactan) - Acrylamide hydrogel

Aye Thwe ThweSoe* and May Myat Khine

Department of Chemical Engineering, West Yangon Technological University, **MYANMAR**

Abstract: There is an increasing need for clean water for human health and the environment, so the removal of toxic metals from wastewater with low-cost adsorbents plays an essential role. In this research, the synthesis of cashew gum (CG) polysaccharide (arabinogalactan)-acrylamide (Am) (CG-AM) hydrogel was carried out with three independent variables: Hydration ratio (ml/g), amount of monomer (acrylamide, Am) (g) and concentration of crosslinker (methylene-bisacrylamide, MBA) (%) by radical polymerisation. The removal efficiency of Pb_{2+} and Cd^{2+} from the stock solution of lead nitrate and cadmium sulphate by adsorption technique was also studied by optimisation using BBD of RSM. Furthermore, the functional and structural properties of all types of hydrogels were analysed by characterisation with FTIR, (XRD), (SEM) with EDS and swelling capacity analysis. An optimum hydrogel yield of 4.527 g was obtained at a hydration ratio of 10 ml/g, monomer amount of 2.5 g and crosslinker concentration of 3% w/v of one gram of extracted arabinogalactan. For Pb^{2+} removal, 86.985 % removal efficiency was obtained at a hydration ratio of 25 ml/g, monomer amount of 1g and crosslinker concentration of 1%, while for Cd2+ removal, 18.875 % removal efficiency was obtained at a hydration ratio of 10 ml/g, monomer amount of 4g and crosslinker concentration of 2%. $(CG\text{-}AM)_H$ Pb^{2+} had the highest swelling capacity of 11.072 g H_2O/g polymer hydrogel but $(CG\text{-}AM)_H$ had the lowest of 5.322 g H_2O/g polymer hydrogel due to crosslinking capacity. The FTIR result, the $(CG\text{-}AM)_H$ Pb^{2+} showed a significant peak of C-O stretching of the S-glycosidic bond of hydrogel to absorb the Pb^{2+} ions. From XRD and SEM results, $(CG\text{-}AM)_H$ Pb^{2+} showed an amorphous nature of hygroscopic properties and a three-dimensional network structure with open pores.

Keywords: Clean water and sanitation; Lead iodide removal; Galactoarabinan; Hydrogel

*Corresponding Author: aythwethwesoe2@gmail.com

Received: May 24th 2024; Revised: August 16th 2024; Accepted: August 19th 2024
https://doi.org/10.58712/jerel.v3i2.156

Reference to this paper should be made as follows: ThweSoe, A. T., & Khine, M. M. (2024). Removal of lead and cadmium from aqueous solution by using cashew gum polysaccharide (Arabinogalactan) - Acrylamide hydrogel. *Journal of Engineering Researcher and Lecturer*, 3(3), 137–158. https://doi.org/10.58712/jerel.v3i2.156

1. Introduction

Water resources around the world are threatened not only by poor industrial management but also by environmental degradation (Mahmoud & Mohamed, 2012). Harmful toxic metals such as lead, cadmium, mercury, copper, zinc and nickel are typically found as hazardous pollutants in industrial effluents in varying concentrations. When these metal ion concentrations accumulate above the allowable limit, they cause environmental safety and public health problems. Therefore, the development of effective removal techniques is essential for water remediation. Among them, the removal of lead and cadmium ions from wastewater plays a vital role in solving environmental pollution problems.

Lead and cadmium are discharged from industrial sectors such as the battery manufacturing process, pigment manufacturing process, printing and photographic materials manufacturing process (Chowdhury et al., 2022). Due to its non-biodegradable nature, it tends to accumulate in the natural environment for a long time (Mahmoud & Mohamed, 2012). In addition, lead causes several types of acute and chronic diseases such as heart attack, and lung cancer and destroys the nervous system of children (Vergili et al., 2017), cadmium irritates the respiratory system, damages the liver, kidney and lungs in human health (Sharma et al., 2021). The widely used methods for metal ion removal are coagulation, adsorption, chemical precipitation, ion exchange, electrodialysis, electrochemical treatment, electrocoagulation and membrane filtration (Bezerra et al., 2008; Mehdipour et al., 2015). The advantages of ion exchange over other methods are high selectivity and simplicity, recovery of required metal ions, low slurry formation and achievement of target limits. Commercial ion exchangers are expensive due to regeneration costs, so research into low-cost adsorbents with high removal rates has been very important (Bezerra et al., 2008).

The application of hydrogel in the agricultural sector, wastewater treatment, pharmaceutical and biomedical purposes such as excipients, drug delivery, wound healing, tissue engineering and cancer therapy has increased in the present day (Anamica & Pande, 2017). Hydrogels are well used as adsorbents as they have better swelling, biocompatibility, functionality surface area etc (Mandal & Ray, 2014). All the applications depend on the properties of the prepared hydrogel. The hydrogel can be prepared from natural polymers with a hydrophilic compound such as hydroxyl, carboxylic acid, and amide either embedded in or grafted onto their polymer backbones (Olorunsola et al., 2016). Chemical crosslinking is a very versatile method for hydrogel preparation that can modify polymers to improve their properties such as mechanical, thermal and chemical stability. Several polysaccharide-based hydrogels have been applied for the adsorption of metal ions in wastewater treatment processes and are of particular interest (Zhao & Mitomo, 2008). Plant gums are hydrophilic, complex polysaccharides with high molecular weight compounds and can form a gel in the presence of solvent or solution due to their gelling ability or ability to improve the viscosity of their dispersions (Choudhary & Pawar, 2014). Exudate gums are one of the oldest natural polysaccharides and are used as thickening and stabilising agents in the food industry. They can form a gel but have poor mechanical and physical properties. To overcome this weakness, they are modified with synthetic monomers such as acrylamide and acrylic acid through network formation by polymerisation reactions to improve binding strength, water retention, flocculation, etc. (Darban et al., 2022).

Cashew tree (*Anacardium occidentale*) family; Anacardiaceae is mainly native to Brazil and cultivated in many tropical and subtropical countries (Soro et al., 2017, 2018). They are also found in many parts of the world, such as Portugal and Asia, India, Nigeria, Kenya, the Philippines and Myanmar. In Myanmar, it is mainly found in the southern part of the country, the Yangon region, where the largest plantation is located. Cashew gum (CG) is a highly hydrophilic plant exudate gum and a complex polysaccharide consisting of 61% galactose, 14% arabinose, 7% rhamnose, 8% glucose, 5% glucuronic acid and 2% other sugar residues. When hydrolysed, they yield L-rhamnose, L-arabinose, D-galactose and glucuronic acid (Ologunagba et al., 2017). The higher amount of monosaccharide; galactose (carbohydrate compound) gives the better galactan structure of the gum to form gels. Arabinogalactan is a polysaccharide formed when hydrogen bonds occur between two molecules of arabinose and galactose (Ma & Johnson, 2023). Arabinogalactan can be used as a tablet binder for pharmaceutical dispersions and as an emulsifier for oil-in-water or water-in-oil emulsions. It is composed of d-glucopyranosyl units either (1 → 6) or (1 → 3) linked with side chains mainly composed of l-arabinofuranose and a small composition of d-galacturonic acid and l-rhamnose. The extraction process is one of the most widely used unit operations industries (Choudhary & Pawar, 2014; Ologunagba et al., 2017).

Acrylamide is a water-soluble polymer and is used as an additive in water treatment, sewage and waste treatment, flocculants, enhanced oil recovery, paper-making aids, thickeners, and soil conditioners. The inspiration of acrylamide affects local impact, irritation of mucous membranes and possible human carcinogens, but the polymerised form of acrylamide is not toxic. Acrylamide is used as a chemical intermediate or as a monomer in the production of polyacrylamide and mainly in the purification of drinking water and the treatment of municipal and industrial wastewater (WHO, 2011). The polyacrylamide hydrogel is prepared in two simultaneous steps, polymerisation and cross-linking. In this study, the polymerisation reaction was carried out using TEMED (tetramethylenediamide) and potassium persulfate (KPS) as the redox initiator pair system and N', N' -methylenebisacrylamide (MBA) as the cross-linking agent (Sousa et al., 2021). The cross-linking of monomer and polymer chains contributes to high swelling capacity, improved mechanical strength and adsorption capacity (Sharma et al., 2021).

Response Surface Methodology (RSM) is an alternative strategy involving a statistical method that could define the effect of the relationship between different parameters. The main advantage of RSM is to reduce the number of experimental trials required to evaluate multiple parameters and their mutual effect. In addition, it is used to improve, advance and optimise reaction processes (Soro et al., 2018). To date, previous studies have been published on the possible application of cashew gum polysaccharide in drug delivery of pharmaceuticals (Kumar et al., 2014) and for biomedical purposes, based hydrogel has been used in the agricultural sector (Sousa et al., 2021). To our knowledge, no study has been reported on cashew gum with acrylamide monomer in hydrogel preparation for heavy metal removal in wastewater treatment. The aim of this study was the synthesis of (CG-AM)H for the removal of Pb^{2+} and Cd^{2+} from a stock solution, using optimisation with Box-Behnken Design (BBD) of RSM. The polysaccharide (arabinogalactan) is extracted from cashew gum (CG). The functional and structural properties of the polysaccharide were studied and the prepared $(CG\text{-}AM)_H$ was also investigated for lead and cadmium removal from a stock solution.

2. Material and methods

2.1 Material

Cashew gum (CG) was collected from a natural source and extracted before use. Acrylamide (AM), N', N' -methylene bisacrylamide (MBA), ammonium persulphate (APS) N', N', N', N'-tetramethyl ethylenediamine (TEMED) of reagent grade were used in the preparation of hydrogel without any other purification. The commercial grade of

96% ethanol was used for the extraction of arabinogalactan from CG. Distilled water (DW) was used as a solvent for the extraction of polysaccharides from cashew gum and redistilled water (RDW) was used as a solvent for the preparation of the required solution preparation in polymerization reaction. Analytical grade of lead nitrate Pb $(NO_3)_2$ and cadmium sulphate Cd (SO_4) was purchased from Academy Group of Co. Ltd of the local market for adsorption experiment.

2.2 Experimental method

2.2.1 Sample collection and preparation

Collection of gum was carried out in the following steps: The trees of cashew (*Anacardium occidentale),* which was grown near the Technological University (Thanlyin) Campus. These exudate gums cashew gum (CG) was collected by tapping the trunks of trees horizontally and left for two weeks. The dried solid bundles of all gum samples were screened by hand to remove pieces of bark and other extra plant materials. Bundles of gums were dried in the hot air oven at 60 ◦C until constant weights to get sufficient solidify brittle condition. Then solid gum samples were ground by a ball mill to reduce solid particle size and sieved through mesh number 100 (<150 μm) to obtain uniform particle size. The samples were sealed in zipped plastic bags for the extraction process.

2.2.2 Extraction process

The polysaccharide compound, arabinogalactan was extracted from CG powder with distilled water (DW) as solvent and optimised using STATISTICA software (Design Expert 7.00). Initially, 5 g of gum powder (150 μm) was hydrated with DW by using a magnetic stirrer at 60 ˚C with 250 rpm for 2hr to obtain a homogeneous dispersion condition. Insoluble parts in the hydration process were removed by the centrifugation process. The dispersion solution was centrifuged at 3000 rpm for 30 min. Two layers, a water-soluble portion and residue appeared in the centrifugation process. The water-soluble portion was precipitated with a precipitating agent: ethanol (96% purity) and kept for 24 hr to complete the precipitation process and the residues were removed. The precipitated polysaccharide was separated by using a vacuum pump under 1 atm pressure for 5 min and washed with DW. The flakes of gum were transferred into the Petri dish and dried in a hot air oven at 60 °C to constant weight. The percentage of yield on a dried basis was measured in triplicate with the initial weight (5 g) of gum powder used in Eq. 1.

$$Yield\ (\%) = \left({}^{M_1}/_{M_2}\right) \times 100 \tag{1}$$

where,

M_1 = mass of the extracted gum powder
M_2 = initial mass of the gum powder

2.2.3 Preparation of polysaccharide hydrogel

The first part of this research was to optimise the amount of yield (gram) of polysaccharide-based hydrogel CG-AM$_H$ by free radical polymerisation method and optimisation was done with BBD. CG$_H$ was prepared as follows: extracted arabinogalactan (1.0 g) was dissolved in RDW until homogeneous condition. A variable amount of monomer (AM) was added. The initiator of APS 5w/v of (5g/100 ml in RDW) and followed by cross-linker (MBA) and 5 w/v TEMED (5g/100 ml in RDW) were added as a redox-initiator pair. The reaction mixture was stirred continuously and heated at 60 °C until the gel state was reached. The polymerisation reaction (5-10 min) was allowed to take place and an acrylamide cross-linked hydrogel was formed. The formed hydrogel was dissolved in RDW for 72 hours to remove unreacted monomers and reagents. The swollen hydrogel was then dried in a hot air oven at 50 °C to obtain constant weight. In the experimental design model, the hydration ratio of redistilled water to polysaccharide (arabinogalactan) for the preparation of the dispersion solution (10ml/g - 40ml/g), the amount of monomer (AM) (1g - 4g), the concentration of crosslinker (MBA) (1% - 3%) in the polymerisation step were taken as three variables of the experiment. The factors of the three variables studied at low, medium and high levels are shown in Table 1.

Table 1. The Level of the selected variables for (CG-AM)$_H$, (CG-AM)$_H$ Pb^{2+}, (CG-AM)$_H$ Cd^{2+}

Variable		**Level**		
		Low	**Medium**	**High**
Hydration ratio (ml/g)	X_1	10	15	40
Monomer Amount (g)	X_2	1	2.5	4
Crosslinker Concentration (%)	X_3	1	2	3

2.2.4 Adsorption experiment

The second part of this research is to optimize the removal percent efficiency of Pb^{2+} and Cd $^{2+}$ from the stock solution of the analytical grade of lead nitrate and cadmium sulphate by adsorption technique with Box-Behnken Design. A concentration of 100 mg/l of lead and cadmium from the stock solution was put into the beaker and 0.2 gram of prepared gel. Fifteen run adsorption experiments from design were carried out by using Jar-Tester with an agitation rate of 120 rpm, agitation time of 180 min and adsorbent dosage was 0.2g/100ml. The pH of the all-solution ranges from pH 5.5-pH 5.9. After the agitation period, the supernatants were filtered with Whatman filter No.4 to avoid metal ions precipitating in the filtrate solution. The initial and final concentrations of the metal solution were measured by Atomic Absorption Spectrometer (AA7000, Shimazu, Japan). The removal efficiency of lead and cadmium was determined by the following equation. Studied three variables' factors of low and high levels were as same as the condition for optimum yield of hydrogel.

$$E\,(\%) = \frac{C_0 - C_1}{C_0} \qquad (2)$$

where,

C_0 = initial concentration of lead (mg/l)
C_1 = final concentration of lead (mg/l)

Table 2. Box-Behnken design matrix of $(CG\text{-}AM)_H$, $(CG\text{-}AM)_H$ Pb^{2+} and $(CG\text{-}AM)_H$ Cd^{2+}

For $(CG\text{-}AM)_H$					For $(CG\text{-}AM)_H$ Pb^{2+}					For $(CG\text{-}AM)_H$ Cd^{2+}				
Run	**Blk**	**A**	**B**	**C**	**Run**	**Blk**	**A**	**B**	**C**	**Run**	**Blk**	**A**	**B**	**C**
1	1	0	1	-1	1	1	0	1	1	1	1	0	0	0
2	1	-1	1	0	2	1	-1	-1	0	2	1	1	1	0
3	1	-1	0	1	3	1	1	0	1	3	1	0	-1	-1
4	1	1	-1	0	4	1	-1	0	-1	4	1	-1	-1	0
5	1	0	0	0	5	1	0	0	0	5	1	1	-1	0
6	1	1	1	0	6	1	-1	1	0	6	1	-1	0	-1
7	1	1	0	-1	7	1	-1	0	1	7	1	0	-1	1
8	1	1	1	1	8	1	1	0	-1	8	1	0	1	-1
9	1	-1	0	0	9	1	0	0	0	9	1	0	0	0
10	1	0	0	0	10	1	0	0	0	10	1	0	1	1
11	1	0	-1	1	11	1	0	-1	-1	11	1	-1	1	0
12	1	0	0	0	12	1	1	1	0	12	1	-1	0	1
13	1	0	1	1	13	1	1	-1	0	13	1	1	0	-1
14	1	-1	0	-1	14	1	0	1	-1	14	1	0	0	0
15	1	0	1	-1	15	1	0	-1	1	15	1	1	0	1

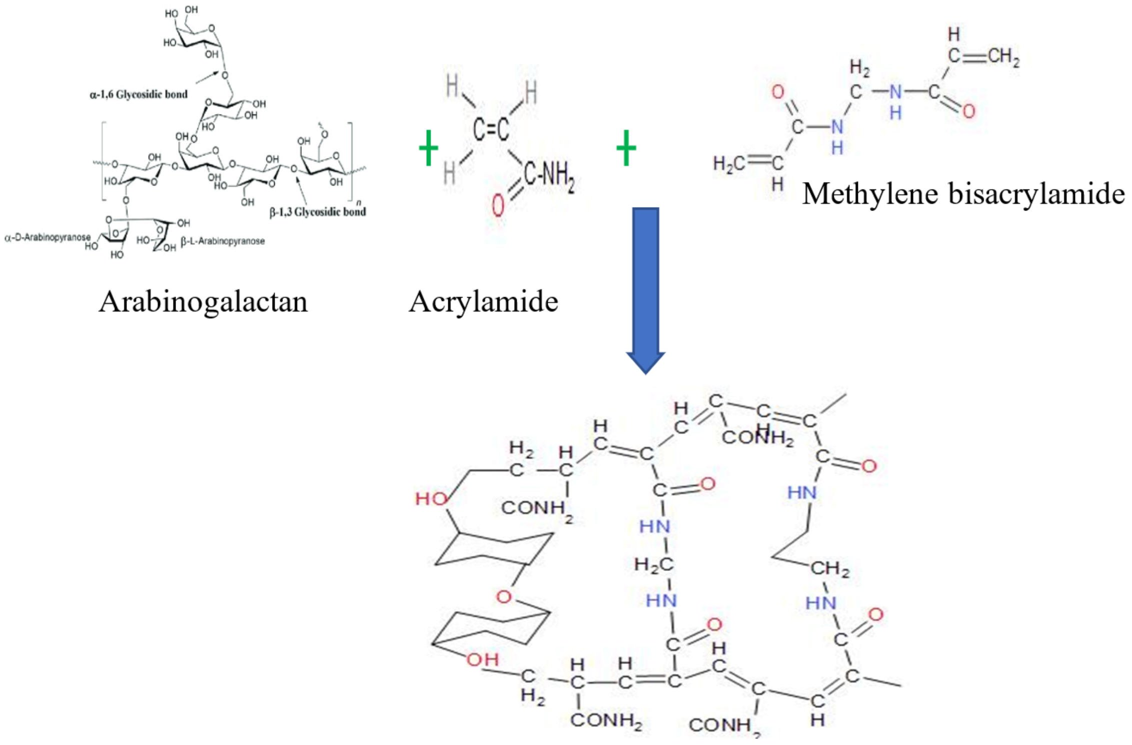

Figure 1. The possible network structure of CG-AM hydrogel by free radical polymerization

2.2.5 Determination of swelling capacity

The swelling capacity of the prepared hydrogels was determined according to the procedure described by Vergili et al. (2017). One gram of hydrogel was immersed in deionized water at room temperature and held for five days until equilibrium swelling was reached. The swollen hydrogel was weighed and the value of the swelling capacity (g of H_2O/g of polymer hydrogel) was calculated in triplicate using Eq. 3.

$$Swelling\ capatity\ \left(g\ of\ \frac{H_2O}{g}\ of\ polymer\ hydrogel\right) = \frac{(W_s - W_d)}{W_d} \tag{3}$$

Where W_s and W_d are the weights of the swollen and dry polymer hydrogel.

2.2.6 Characterization techniques

The prepared CG-Am hydrogel was characterized using FTIR, XRD and SEM for its functional and structural properties.

2.2.6.1 Fourier Transform Infrared Spectra (FITR)

The FT-IR spectra were used to inform on functional groups. The presence of a functional group in the before and after adsorption experiment was determined by using a Thermo Fisher Scientific, Summit PRO FTIR Spectrophotometer (USA) with a wavelength range of 500- 4000 cm^{-1}.

2.2.6.2 X-ray diffraction (XRD)

The XRD pattern analysis for determination of sample purity was using the Rigaku X-ray diffractometer, Japan with a 2 theta range of 10º-80º.

2.2.6.3 Scanning Electron Microscope (SEM)

For examination of The morphology of the hydrogel surface before and after the adsorption process was observed by using a scanning electron microscope JEOL (JSM IT-2000, Japan) vacuum pressure with argon gas by coating with a thin layer of gold about $1\mu m$ of dispersion in a sample holder of 1-1.2 cm diameter.

3. Results and discussion

Statistical design was an effective tool for determining the influence of parameters on the process behaviour. RSM is an accurate statistical technique for designing experiments, building models, analysing the effect of factors and finding optimum conditions for the required response. In this study, the Box-Behnken design was used to investigate the interaction between the selected variable factors. The experimental values of the response: amount of hydrogel (g) and removal efficiency (%) are shown in Tables 3, 4 and 5.

Table 3. Amount of (CG-AM)$_H$ (g) from design of experiment

Std Order	Run Order	Pt Type	Blocks	Hydration Ratio (ml/g)	Monomer Amount (g)	Crosslinker Concentration (%)	Hydrogel Amount (g)
7	1	2	1	10	2.5	3	4.527
6	2	2	1	40	2.5	1	3.842
3	3	2	1	10	4	2	4.004
10	4	2	1	25	4	1	4.192
12	5	2	1	25	4	3	4.429
14	6	0	1	25	2.5	2	3.628
8	7	2	1	40	2.5	3	3.452
4	8	2	1	40	4	2	3.374
2	9	2	1	40	1	2	1.362
13	10	0	1	25	2.5	2	3.909
15	11	0	1	25	2.5	2	3.681
11	12	2	1	25	1	3	1.643
9	13	2	1	25	1	1	2.406
5	14	2	1	10	2.5	1	3.305
1	15	2	1	10	1	2	1.503

Table 4. Value of Pb^{2+} removal (%) from the design of experiment for (CG-AM)$_H$ Pb^{2+}

Std Order	Run Order	Pt Type	Blocks	Hydration Ratio (ml/g)	Monomer Amount (g)	Crosslinker Concentration (%)	% Removal
12	1	2	1	25	4	3	28.635
1	2	2	1	10	1	2	69.765
8	3	2	1	40	2.5	3	14.835
5	4	2	1	10	2.5	1	42.5
14	5	0	1	25	2.5	2	31.78
3	6	2	1	10	4	2	16.66
7	7	2	1	10	2.5	3	22.36
6	8	2	1	40	2.5	1	18.145
15	9	0	1	25	2.5	2	32.045
13	10	0	1	25	2.5	2	30.13
9	11	2	1	25	1	1	86.985
4	12	2	1	40	4	2	19.625
2	13	2	1	40	1	2	44.185
10	14	2	1	25	4	1	26.595
11	15	2	1	25	1	3	50.755

Table 5. Value of Cd^{2+} removal (%) from the design of experiment for (CG-AM)$_H$ Cd^{2+}

Std Order	Run Order	Pt Type	Blocks	Hydration Ratio (ml/g)	Monomer Amount (g)	Crosslinker Concentration (%)	% Removal
13	1	0	1	25	2.5	2	18.235
9	2	2	1	25	1	1	9.75
12	3	2	1	25	4	3	16.059
10	4	2	1	25	4	1	8.706
7	5	2	1	10	2.5	3	16.125
8	6	2	1	40	2.5	3	10.75
1	7	2	1	10	1	2	6.029
15	8	0	1	25	2.5	2	16.823
2	9	2	1	40	1	2	9.00
4	10	2	1	40	4	2	10.265
11	11	2	1	25	1	3	9.583
14	12	0	1	25	2.5	2	15.853
3	13	2	1	10	4	2	18.875
6	14	2	1	40	2.5	1	14.853
5	15	2	1	10	2.5	1	11

In order to demonstrate the correlation between the independent and dependent variables, three-dimensional (3D) plots and two-dimensional (2D) plots were used to define the response in function. In this study, the response surface (3D) and contour plot (2D) which represent the interrelation effect of the selected variable three factors (hydration ratio, monomer amount and crosslinker concentration) for hydrogel yield and percentage removal of Pb^{2+} were shown in Figure 2, 3, 4, and 5.

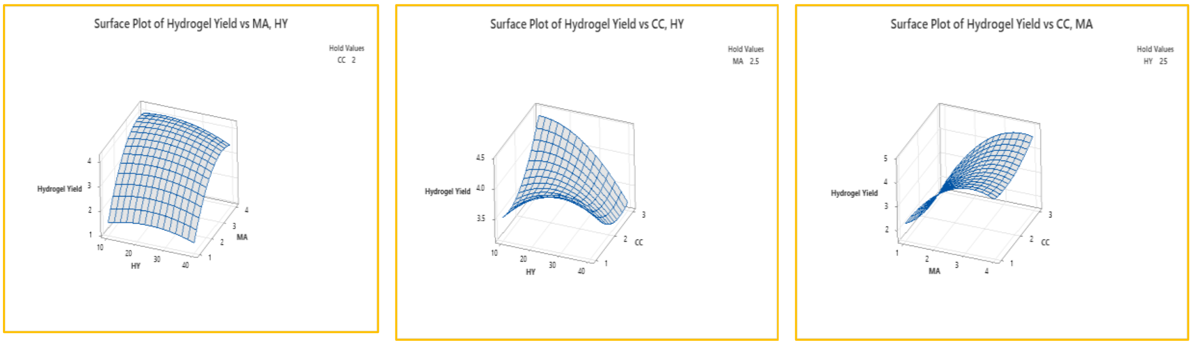

(a) (b) (c)

Figure 2. Response Surface plot showing the effect of monomer amount and hydration ratio. (a) Crosslinker concentration and hydration ratio, (b) Crosslinker concentration and monomer amount, and (c) on $(CG\text{-}AM)_H$ Yield

Therefore, the response surface (Fig. 2a) and the contour plot (Fig. 3a), represent the amount of hydrogel yield (gram) as a function of Hydration Ratio (X_1) and Monomer Amount (X_2) with fixed at Crosslinker Concentration (X_3) fixed at (2%) (level 1) and showed that the amount of hydrogel yield increased when hydration ratio and Monomer amount increased in the range 10-40 ml/g and from 1-4g. Hydration Ratio (X_1) and Crosslinker Concentration (X_3) with Monomer Amount (X_2) (2.5g) (level 0), were also illustrated by the 3D (Fig. 2b) and 2D (Fig. 3b) graphical representations. The analysis of Fig. 1b showed that the CG_H yield increased when hydration ratio (X_1) and Crosslinker Concentration (X_3) increased in the range of 10-38 ml/g and 1-1.5% respectively; but beyond 38 ml/g and 1.5%, yield amount decreased slightly. In Figure 1c and Figure 3c, the amount of yield increased when the Monomer amount increased and Crosslinker Concentration decreased from 4-1g and 3-1% respectively with the amount of hydration ration held at 25ml/g.

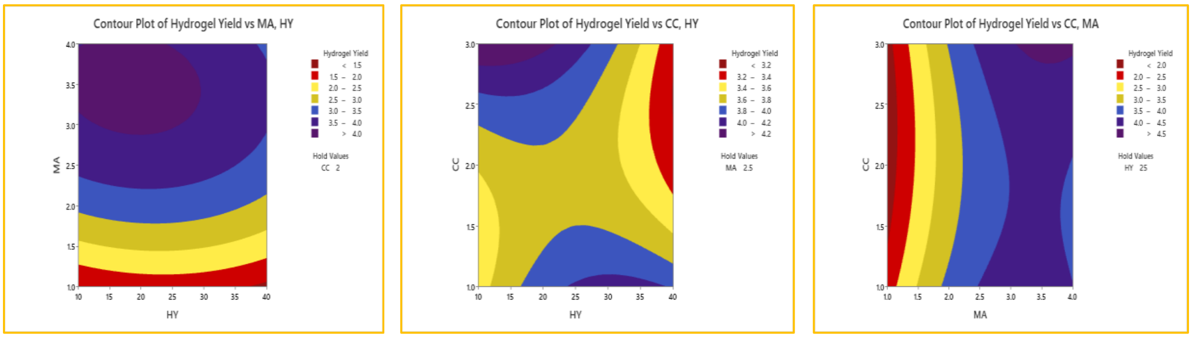

(a) (b) (c)

Figure. 3 Contour plot showing the effect of monomer amount and hydration ratio. (a) Crosslinker concentration and hydration ratio, (b) Crosslinker concentration and monomer amount, and (c) on $(CG\text{-}AM)_H$ Yield

The response surface (Fig. 4a) and the contour plot (Fig. 5a), represent the efficiency of the percentage of lead removal (%) as a function of Hydration Ratio (X_1) and Monomer Amount (X_2) with fixed at Crosslinker Concentration (X_3) fixed at (2%) (level 1), and showed that Removal Efficiency % of Pb^{2+} increased when hydration ratio and Monomer amount decreased from 28-10 ml/g and 1.25g - 1g respectively, but below 28ml/g and 1.25g, removal percent decreased. Hydration Ratio (X_1) and Crosslinker Concentration (X_3) with Monomer Amount (X_2) (2.5g) (level 0), were also displayed by the 3D (Fig. 4b) and 2D (Fig. 5b) graphical illustrations. The analysis of Fig. 1b showed that the Removal % increased when hydration ratio (X_1) and Crosslinker Concentration (X_3) increased in the range of 10-15 ml/g and 1% respectively; but beyond 15 ml/g and 1%, Removal % decreased slightly. In Figure 3c and Figure 4c, the Removal Efficiency % of Pb increased when the Monomer amount and Crosslinker Concentration decreased from 4-1g and 3-1% respectively with the amount of hydration ration held at 25ml/g. This showed that the effect of Monomer amount (X_2) and Crosslinker Concentration (X_3) on the Removal Efficiency % of Pb is significant. Moreover, the elliptical contour plots in Fig. 5c mean that there is a significant mutual interaction between the two variables Monomer Amount (X_2) and Crosslinker Concentration (X_3).

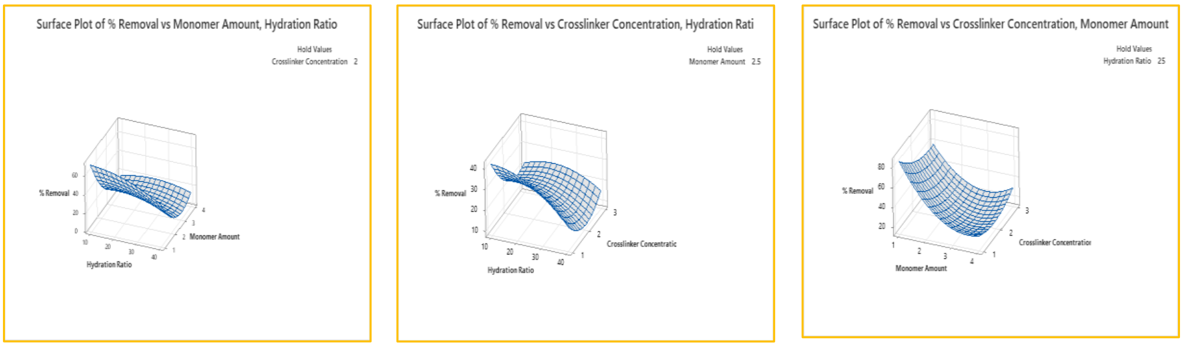

(a) (b) (c)

Figure 4. Response Surface plot showing the effect of monomer amount and hydration ratio. (a) Crosslinker concentration and hydration ratio, (b) Crosslinker concentration and monomer amount, and (c) on $(CG\text{-}AM)_H$ for Pb^{2+} removal

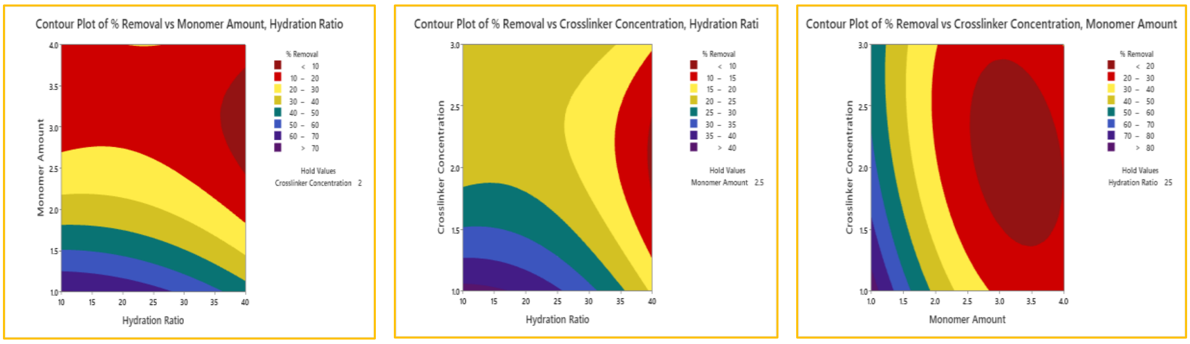

(a) (b) (c)

Figure 5. Contour plot showing the effect of monomer amount and hydration ratio. (a) Crosslinker concentration and hydration ratio, (b) Crosslinker concentration and monomer amount, and (c) on $(CG\text{-}AM)_H$ for Pb^{2+} removal

The response surface (Fig. 6a) and the contour plot (Fig. 7a), represent the efficiency of the percentage of lead removal (%) as a function of Hydration Ratio (X_1) and

Monomer Amount (X_2) with fixed at Crosslinker Concentration (X_3) fixed at (2%) (level 1) and showed that Removal Efficiency % of Cd^{2+} increased when hydration ratio and Monomer amount increased, but beyond 31ml/g of hydration, ratio removal percent decreased. Hydration Ratio (X_1) and Crosslinker Concentration (X_3) with Monomer Amount (X_2) (2.5g) (level 0), were also illustrated by the 3D (Fig. 6b) and 2D (Fig. 7b) graphical representations. The analysis of Fig. 7b showed that the Removal % increased when the hydration ratio (X_1) and Crosslinker Concentration (X_3) increased in the range of 10-31 ml/g and 1-3% respectively, but beyond 31 ml/g decreased slightly. In Figure 6c and Figure 7c, the Removal Efficiency % of Cd^{2+} increased when the Monomer amount and Crosslinker Concentration increased from 1-4g and 1-3% respectively with the amount of hydration ration held at 25ml/g. This showed that the effect of hydration ratio (X_1), Monomer amount (X_2) and Crosslinker Concentration (X_3) on Removal Efficiency % of Cd^{2+} is significant. Moreover, the elliptical contour plots in Figures 7b and 7c mean that there is a significant mutual interaction between the three variables hydration ratio (X_1), Monomer Amount (X_2) and Crosslinker Concentration (X_3).

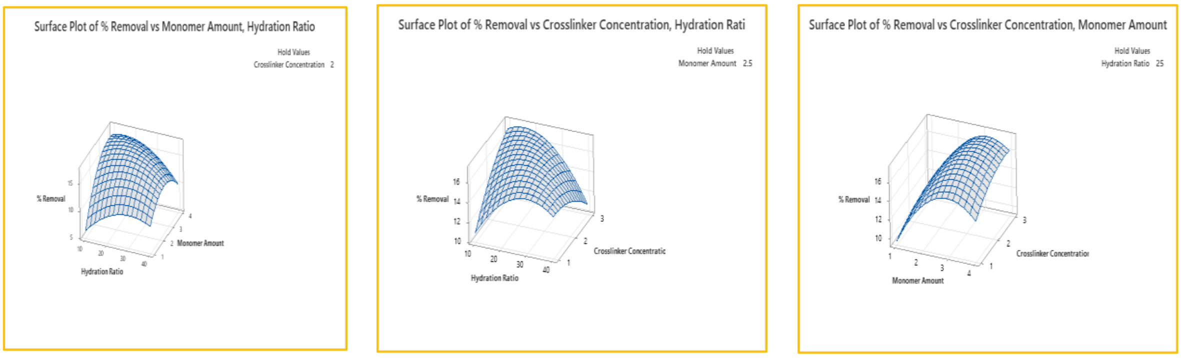

(a) (b) (c)

Figure 6. Response Surface plot showing the effect of monomer amount and hydration ratio. (a) Crosslinker concentration and hydration ratio, (b) Crosslinker concentration and monomer amount, and (c) on $(CG\text{-}AM)_H$ for Cd^{2+} removal

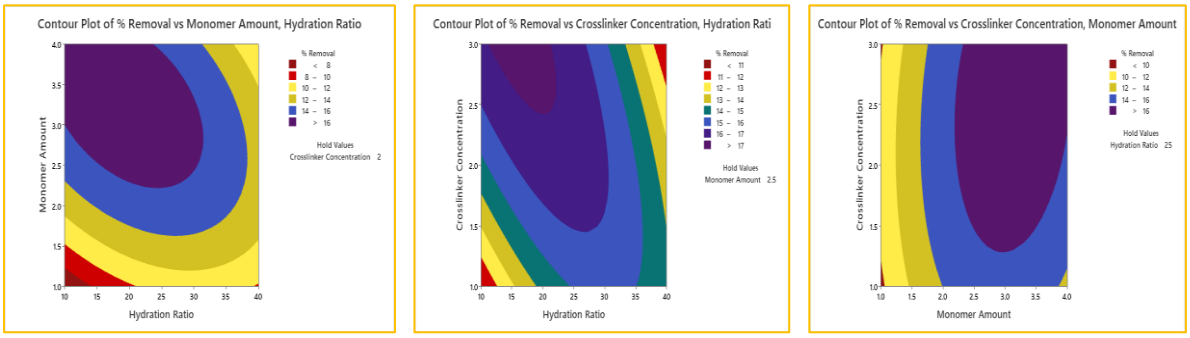

(a) (b) (c)

Figure 7. Contour plot showing the effect of monomer amount and hydration ratio. (a) Crosslinker concentration and hydration ratio, (b) Crosslinker concentration and monomer amount, and (c) on $(CG\text{-}AM)_H$ for Cd^{2+} removal

Whether the prepared design model was well fitted to variable parameters, the statistical significance of the mean square ratio variation due to regression and residual errors of the mean square were evaluated using the ANOVA technique (Soro et al., 2018). The analysis of variance (ANOVA) which was tested for the prepared design was presented in Tables 6, 7 and 8.

Table 6. Analysis of variance for the design of yield of (CG-AM)$_H$

Source	**DF**	**Adj SS**	**Adj MS**	**F - value**	**P - Value**	**R^2 Value**	**Adj R^2**	**Predict R^2**
Model	9	15.2611	1.6957	30.03	0.001	98.18%	94.91%	74.88%
Error	5	0.2823	0.0565					
Lack-of-Fit	3	0.2377	0.0792					
Pure Error	2	0.0446	0.0223					
Total	14	15.5434						

Table 7. Analysis of variance for the design of (CG-AM)$_H$ Pb^{2+} for Pb removal

Source	**DF**	**Adj SS**	**Adj MS**	**F - value**	**P - Value**	**R^2 Value**	**Adj R^2**	**Predict R^2**
Model	9	6699.70	744.41	112.60	0.000	99.51%	98.63%	92.77%
Error	5	33.06	6.61					
Lack-of-Fit	3	30.01	10.00	6.57	0.135			
Pure Error	2	3.05	1.52					
Total	14	6732.76						

Table 8. Analysis of variance for the design of (CG-AM)$_H$ Cd^{2+} for Cd removal

Source	**DF**	**Adj SS**	**Adj MS**	**F - value**	**P - Value**	**R^2 Value**	**Adj R^2**	**Predict R^2**
Model	9	171.027	17.003	18.23	0.003	97.04%	91.72%	59.51%
Error	5	5.211	1.0423					
Lack-of-Fit	3	4.336	1.4455					
Pure Error	2	0.875	0.4374					
Total	14	176.239						

For designing both (CG-AM)$_H$, and (CG-AM)$_H$ for Pb^{2+} and Cd^{2+}, the coefficient of determination (R^2) and the adjusted determination coefficient (adj-R^2) were nearly approached. If the model fitted the experimental data well, the value of (R^2) and the adjusted value (adj-R^2) were nearly approaching unity. For models fitted for CG$_H$, (R^2) was 98.18%, which showed that 1.82% of the total variations were not defined by the model (Table 6). The p-value of the model ($p<0.05$) was 0.001 suggesting that the model was significant. For CG$_H$ Pb^{2+}, (R^2) was 99.51%, which showed that only a coefficient of variation of 0.49% was not defined by the model (Table 7). The p-value of the model ($p<0.05$) was 0.000 suggesting that the model was significant. Moreover, the value of the adjusted determination coefficient (adj-R^2 = 98.63%) also verified that the model was highly significant. For CG$_H$ Cd^{2+}, (R^2) was 97.04%, which showed that 2.96% of the total variations were not defined by the model (Table 8). Correlation between the study factors on the response of yield was shown in first-order and second-order polynomial equations (4) and (5) for CG$_H$, and Eq. (6) and (7) for CG$_H$ Pb^{2+} and Eq. (8) and (9) for CG$_H$ Cd^{2+}.

$$Y = 3.739 - 0.1636X_1 + 0.1356X_2 + 0.0383X_3 \tag{4}$$

$$\mathrm{Y} = 3.79 - 0.282\mathrm{X}_1{}^2 - 0.896\mathrm{X}_2{}^2 + 0.324\mathrm{X}_3{}^3 - 0.122\mathrm{X}_1\mathrm{X}_2 - 0.403\mathrm{X}_1\mathrm{X}_3 + 0.25\mathrm{X}_2\mathrm{X}_4 \quad (5)$$

where Y is the yield of hydrogel.

$$Y = 31.32 - 6.812X_1 - 20.022X_2 - 7.205X_3 \quad (6)$$

$$\mathrm{Y} = 31.32 - 8.77\mathrm{X}_1{}^2 - 15.01\mathrm{X}_2{}^2 + 1.91\mathrm{X}_3{}^3 + 7.14\mathrm{X}_1\mathrm{X}_2 - 4.21\mathrm{X}_1\mathrm{X}_3 + 9.57\,\mathrm{X}_2\mathrm{X}_4 \quad (7)$$

where Y is the removal % of Pb^{2+}.

$$Y = 16.603 - 0.676X_1 + 2.568X_2 + 0.682X_3 \quad (8)$$

$$\mathrm{Y} = 16.603 - 2.556\mathrm{X}_1{}^2 - 3.442\mathrm{X}_2{}^2 - 0.865\mathrm{X}_3{}^3 - 2.458\,\mathrm{X}_1\mathrm{X}_2 - 2.307\mathrm{X}_1\mathrm{X}_3 + 0.608\mathrm{X}_2\mathrm{X}_4 \quad (9)$$

where Y is the removal of Cd^{2+}.

According to the design of the experiment, in $(CG\text{-}AM)_H$ for yield increasing the amount of monomer and the concentration of crosslinker increased the yield amount of $(CG\text{-}AM)_H$ but the required amount of hydration was low for dispersing solution preparation. When the required amount of hydration is higher, hydrogel yield decreases because the extra amount of water causes a low degree of crosslinking to form the hydrogel. Therefore, the use of crosslinker was an important factor in proper crosslinking of hydrogel preparation. For removing lead, the highest removal percentage was found at lower monomer amount and lesser concentration of crosslinker.

3.1 Swelling capacity analysis

The swelling capacity is related to the mobility and crosslinking degree of the polymer chain. The swelling capacity decreases with increased crosslinking. Higher swelling capacity means more water contained in the polymer molecular chains (Ma & Johnson, 2023). The equilibrium swelling capacity values of $(CG\text{-}AM)_H$, $(CG\text{-}AM)_H$ Pb^{2+} and $(CG\text{-}AM)_H$ Cd^{2+} were found to be 5.322, 11.072g and 5.636g of water/ g of polymer, respectively. The lower level of crosslinking increases the swelling properties of the prepared gel and more metal ions are trapped in the hydrogel's swelling surface.

3.2 Functional analysis

Functional analysis was performed to determine the presence of compounds. The analysed functional groups of the hydrogel samples are shown in Figure 8. The results of FTIR spectra of arabinogalactan, $(CG\text{-}AM)_H$, $(CG\text{-}AM)_H$ Pb^{2+} and $(CG\text{-}AM)_H$ Cd^{2+} before and after adsorption were presented in Figure 8. FTIR spectra showed major peaks at 3185 cm^{-1}, 2926 cm^{-1}, 1656 cm^{-1}, 1425 cm^{-1}, 1350 cm^{-1}, 1280 cm^{-1} and 1081 cm^{-1} in $(CG\text{-}AM)_H$ for yield, corresponding to 3333 cm^{-1}, 3193 cm, 1655 cm^{-1}, 1417 cm^{-1}, 1324 cm^{-1}, 1072 cm^{-1} before adsorption and 3334 cm^{-1}, 3190 cm, 2924 cm^{-1}, 1650 cm^{-1}, 1452 cm^{-1}, 1416 cm^{-1},1080 cm^{-1} peaks of $(CG\text{-}AM)_H$ Pb^{2+} after Pb^{2+} adsorption respectively. It displays a prominent band at 3300 cm^{-1} of $(CG\text{-}AM)_H$ revealing the stretching vibrations for the -OH groups of carboxylic acid. The amide and amine group of the peak for the C-H stretching vibrations present both $(CG\text{-}AM)_H$ Pb^{2+} and $(CG\text{-}AM)_H$ Cd^{2+} was detected at 2924 cm^{-1} before adsorption and shift to 2933 cm^{-1} and 2930 cm^{-1} after adsorption. The symmetrical stretching for the peaks at 1646 cm^{-1} and 1605 cm^{-1} for hydrogel yield and 1650 cm^{-1} and 1600 cm^{-1} are owing to the stretching of carbonyl groups and reveal carboxylate groups of polyacrylamides (Bezerra et al., 2008). Thus, these peaks are indicative of the C=O groups present in both types of gel (Kannan & Seenivasan, 2006). The appearance and intensification of the two peaks at 1411 cm$^{−1}$ and 1318 cm$^{−1}$ for the primary NH_2 groups confirmed that AR-Am chains grew on the polymer backbone (Mansoorian et al., 2014).

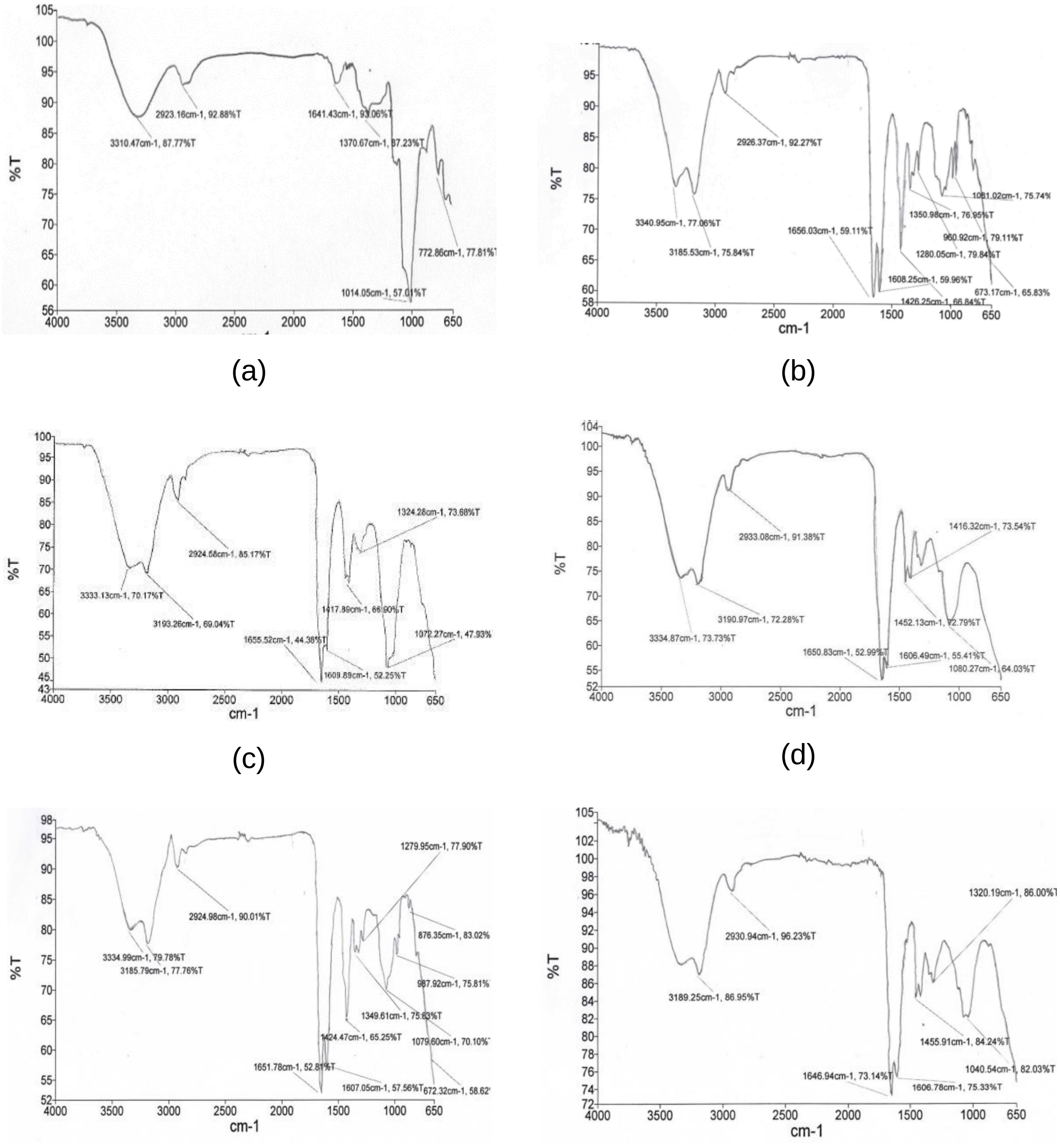

(a) (b)

(c) (d)

(e) (f)

Figure. 8 FTIR spectra of (a) Extracted CG (arabinogalactan), (b) (CG-AM)$_H$ for Yield, (c) (CG-AM)$_H$ Pb^{2+} before adsorption, (d) after adsorption, (e) (CG-AM)$_H$ Cd^{2+} before adsorption, and (f) after adsorption

The band at 1036 cm^{-1} announce the stretching of the C-O bond of glycosidic bonds. The appearance of a peak at 1097cm$^{−1}$ and a shoulder in hydrogel yield proved that longer polyacrylamide chains were seen in hydrogel yield (Mansoorian et al., 2014). The longer polyacrylamide chains will push high crosslink ability. After the adsorption of Pb^{2+} ions, the long and strong peaks of the C-O bond of glycosidic bonds change to short and broad peaks with slight variations in peak intensities due to the intermolecular mutual action between the hydrogel and Pb^{2+} ions. Moreover, the formation of the shoulder was longer polyacrylamide chains due to the occupying of Pb^{2+} ions in the prepared gel. After the adsorption of Cd^{2+} ions, CG_H Cd^{2+} had one long sharp peak at 1424 cm^{-1} and one significant peak at 1079 cm^{-1} was changed to short and broad due to the intermolecular interactions between the hydrogel and Cd^{2+} ions. The disappearance of the peak at 987 cm^{-1} was due to the crosslinking network of the gel. Thus, it can be concluded that the changes in the FTIR spectrum of hydrogel after Pb^{2+} ion adsorption are due to the physicochemical interactions of the polymeric network and Pb^{2+} ion.

3.3 X-ray diffraction (XRD) analysis

To study the crystallinity and amorphous nature of hydrogel samples, the X-ray Diffraction (XRD) analysis was performed. The resulting XRD pattern which affects the nature of polysaccharide, polysaccharide-based hydrogel was borne in Figure 9. According to the XRD pattern, the broad diffused centre peak at $2\theta = 18.16°$ was found in extracted arabinogalactan which expresses a material with a low degree of structural properties. The XRD pattern of the CG_H for yield and CG_H Pb^{2+} showed a distinct, broad diffused centre peak at $2\theta = 21.81°$ at intensity count 213 and $2\theta = 21.31°$ at intensity count 173 that showed the amorphous nature of the polymeric matrix (ALSamman & Sánchez, 2023). Except for CG_H Cd^{2+}, the XRD pattern of all types of prepared hydrogels had a broad diffraction peak at 2θ about 20 Madegree and that indicated the amorphous nature of polyacrylamide hydrogel. XRD results are consistent with the literature for the XRD pattern of polyacrylamide hydrogel with amorphous nature (El Amri et al., 2022). The amorphous structure of hydrogel shows more hygroscopic properties than the crystalline structure with high purity and soluble in nature. For CG_H Cd^{2+}, there were six distinct sharp peaks 2θ at 11.19, 19.33, 19.46, 20.67, 24.03, 28.64 degree with acrylamide crystalline structure due to the addition of the higher amount of monomer (AM) and monomer was not completely removed in hydrogel preparation (Trivedi et al., 2015).

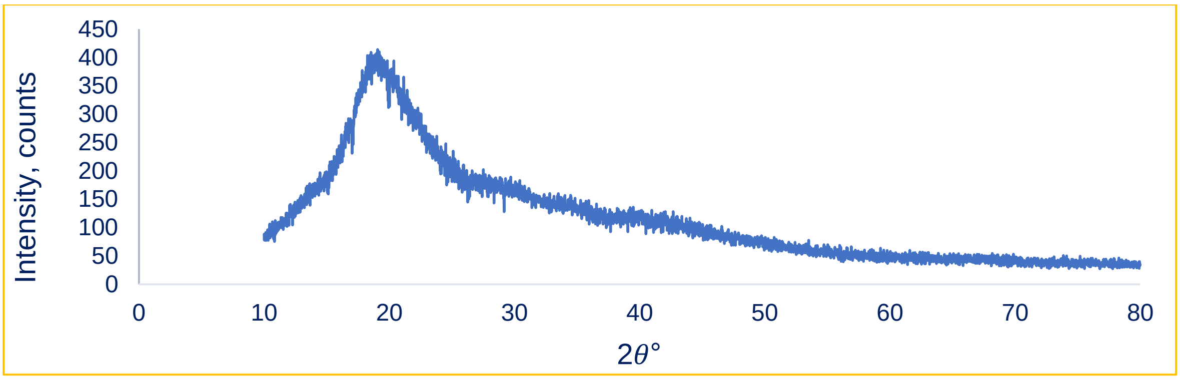

(a)

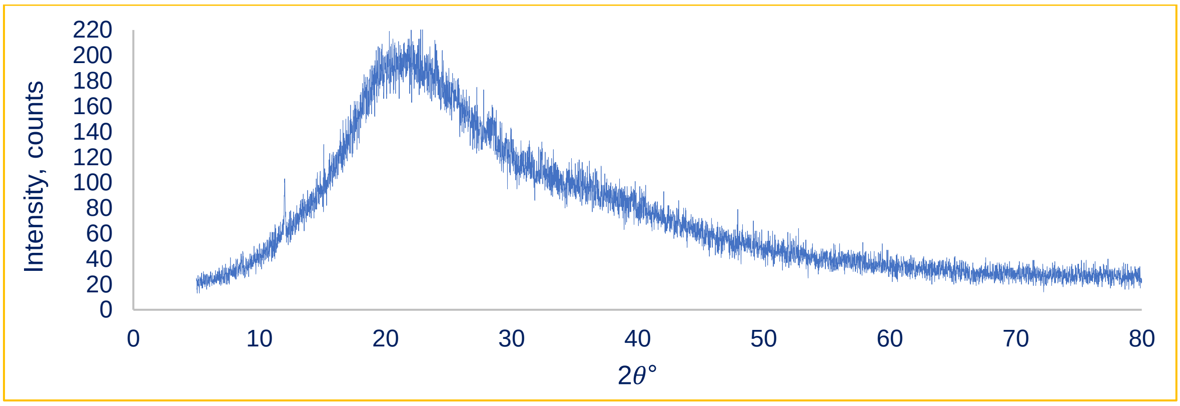

(b)

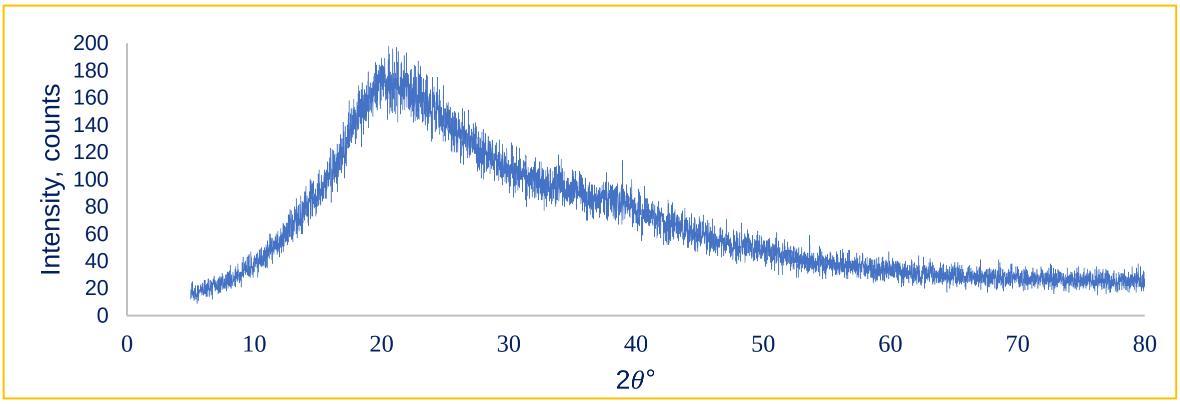

(c)

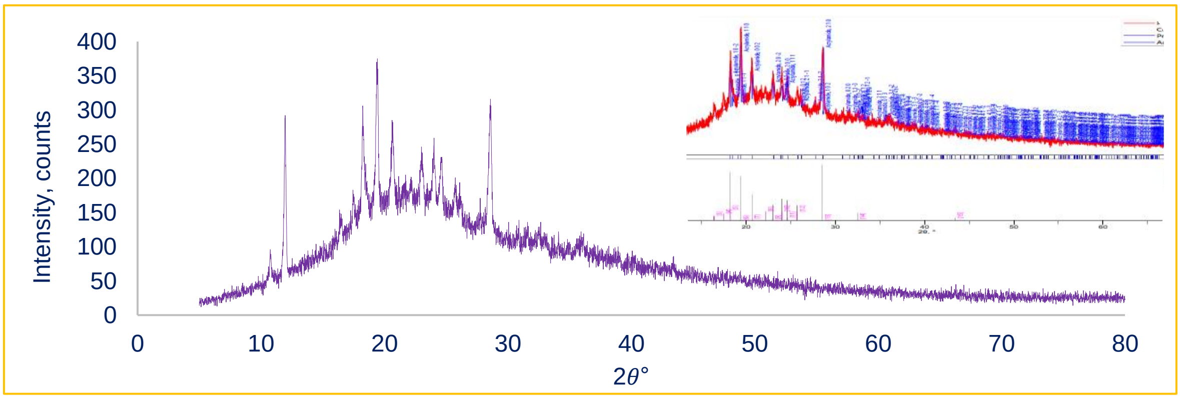

(d)

Figure 9. XRD pattern of (a) Extracted Polysaccharide (arabinogalactan), (b) $(CG\text{-}AM)_H$ (c) $(CG\text{-}AM)_H$ Pb^{2+}, and (d) $(CG\text{-}AM)_H$ Cd^{2+}

3.4 Scanning Electron Microscopy (SEM) analysis

SEM was used to explore the morphology formation of arabinogalactan, $(CG\text{-}AM)_H$. $(CG\text{-}AM)_H$ Pb^{2+} and $(CG\text{-}AM)_H$ Cd^{2+} before and after adsorption (Barros et al., 2023). Fractured and pores nature was observed in the extraction of arabinogalactan from CG (Fig. 10 a). It appears that the morphological nature of crosslinked hydrogels was changed to flaky layers because of crosslinked network formation. In the SEM images of $(CG\text{-}AM)_H$ Pb^{2+} at 1000 magnification (Fig. 10e), it can be seen that the surface texture was significantly distinct from that of $(CG\text{-}AM)_H$ for yield, and indicating that it was a three-dimensional network crosslinked formation with pore pattern and open channel was observed which indicates it can entrap the metal Pb^{2+} ion in the polymer hydrogel's network like a porous membrane for adsorption process. The formation of pores and voids in the gels had a significant effect on the surface morphology of the superabsorbent material (Barros et al., 2023). The high porosity of flake and bloom with open channel pores appeared throughout the morphology structure of $(CG\text{-}AM)_H$ Cd^{2+} showing the metal ion can combine with the functional group on the surface. After the adsorption process, the morphology of $(CG\text{-}AM)_H$ Pb^{2+} was changed to aggregation type and slice type for $(CG\text{-}AM)_H$ Cd^{2+} and the distinct white spot with a smooth surface occurred which may be due to the implication of metal ion to the hydrogel surface.

The EDS result was completed to examine the chemical composition of the prepared hydrogel sample's surface (ALSamman & Sánchez, 2023). The presence of oxygen(O) and sulphur (S) because of the presence of sulfur linkage glycosidic bond of hydrogel (*Glycoside - Wikipedia*, n.d.) and identified peak of Lead (Pb^{2+}) in $(CG\text{-}AM)_H$ Pb^{2+} due to the interaction of carboxylate $(COO)^-$ and sulphate (SO_4-) with lead (Pb+) metal with highest mass percentage of 63.96. The presence of carbon (C), nitrogen (N) and Oxygen (O) discovered peak of Cadmium (Cd) in $(CG\text{-}AM)_H$ for Cd^{2+} formation was due to the interaction of carboxylate $(COO)^-$ and nitrate (NO_3-) and with Cadmium (Cd+) metal with the mass percentage of 0.5.

From SEM and EDS results, the mass percentage of Pb^{2+} ion on $(CG\text{-}AM)_H$ Pb^{2+} surface was significantly higher than for Cd^{2+} ion on $(CG\text{-}AM)_H$ Cd^{2+} because of the higher atomic mass 207.2 g/mole with smaller atomic size 0.175 nm of Pb^{2+} ion and lower atomic mass 112.414 g/mole with higher atomic size 0.154nm of Cd^{2+} ion.

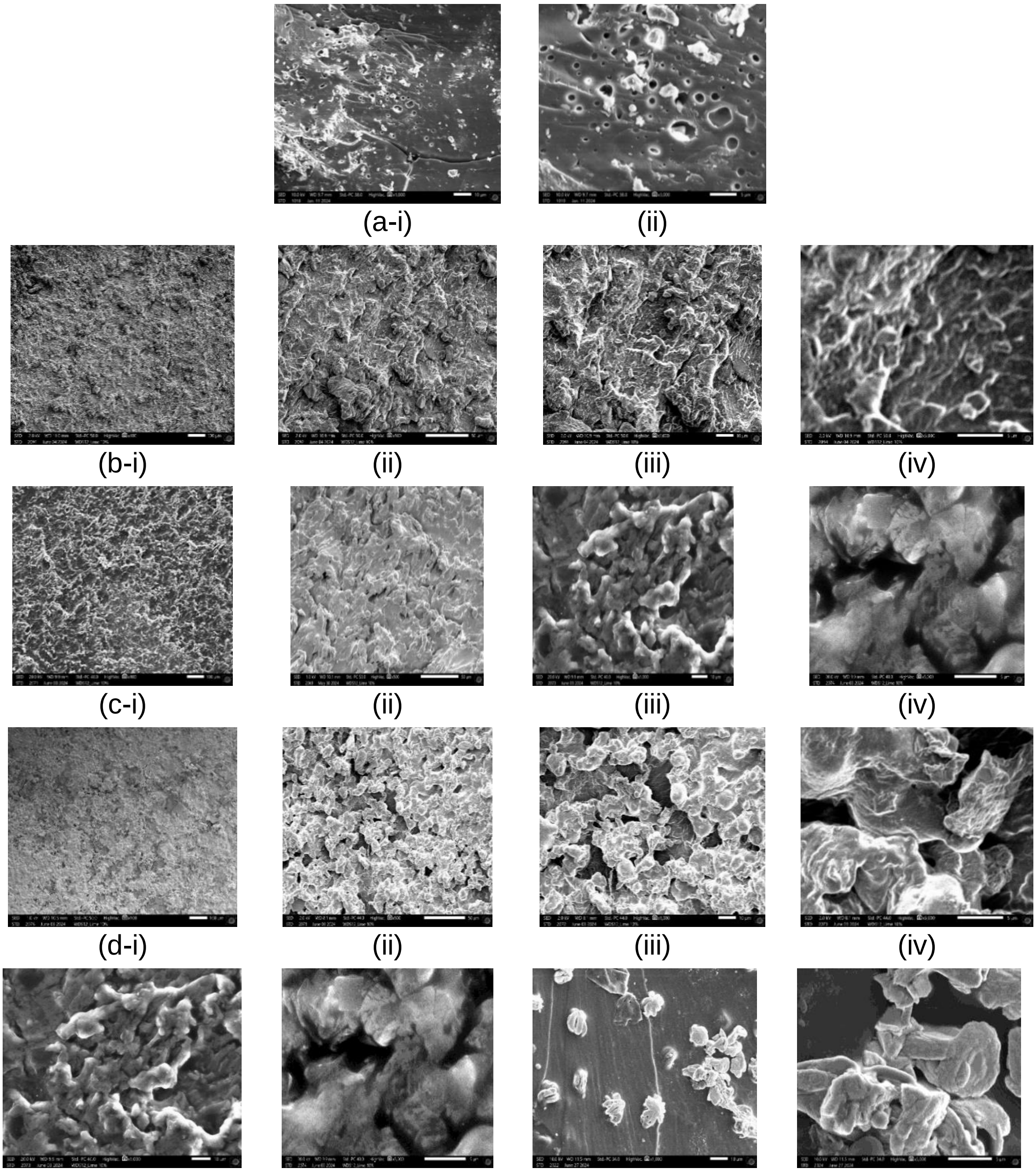

(a-i) (ii)

(b-i) (ii) (iii) (iv)

(c-i) (ii) (iii) (iv)

(d-i) (ii) (iii) (iv)

(e-i) before treatment (ii) after treatment

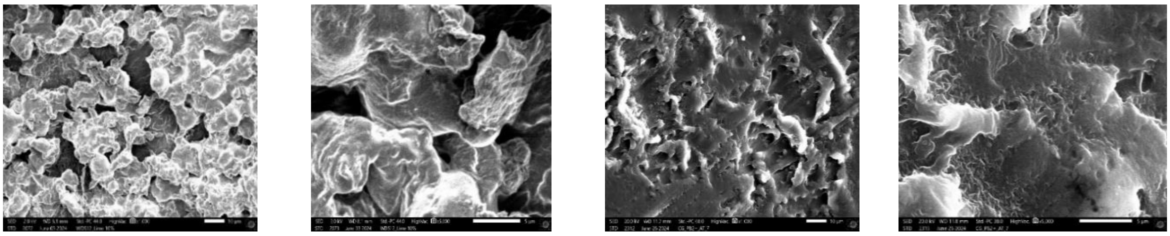

(f-i) before treatment (ii) after treatment

Figure 10. SEM image of extracted arabinogalactan (x1000,3000) (a-i, ii), (CG-AM)$_H$ (x100,500,1000,5000) (b-i, ii, iii, iv), (CG-AM)$_H$ Pb^{2+} and (CG-AM)$_H$ Cd^{2+} before adsorption (x100,500,1000,5000) (c-i, ii, iii, iv) & (d-i, ii, iii, iv), after adsorption (x1000,5000) (e-i, ii), (f-i, ii,)

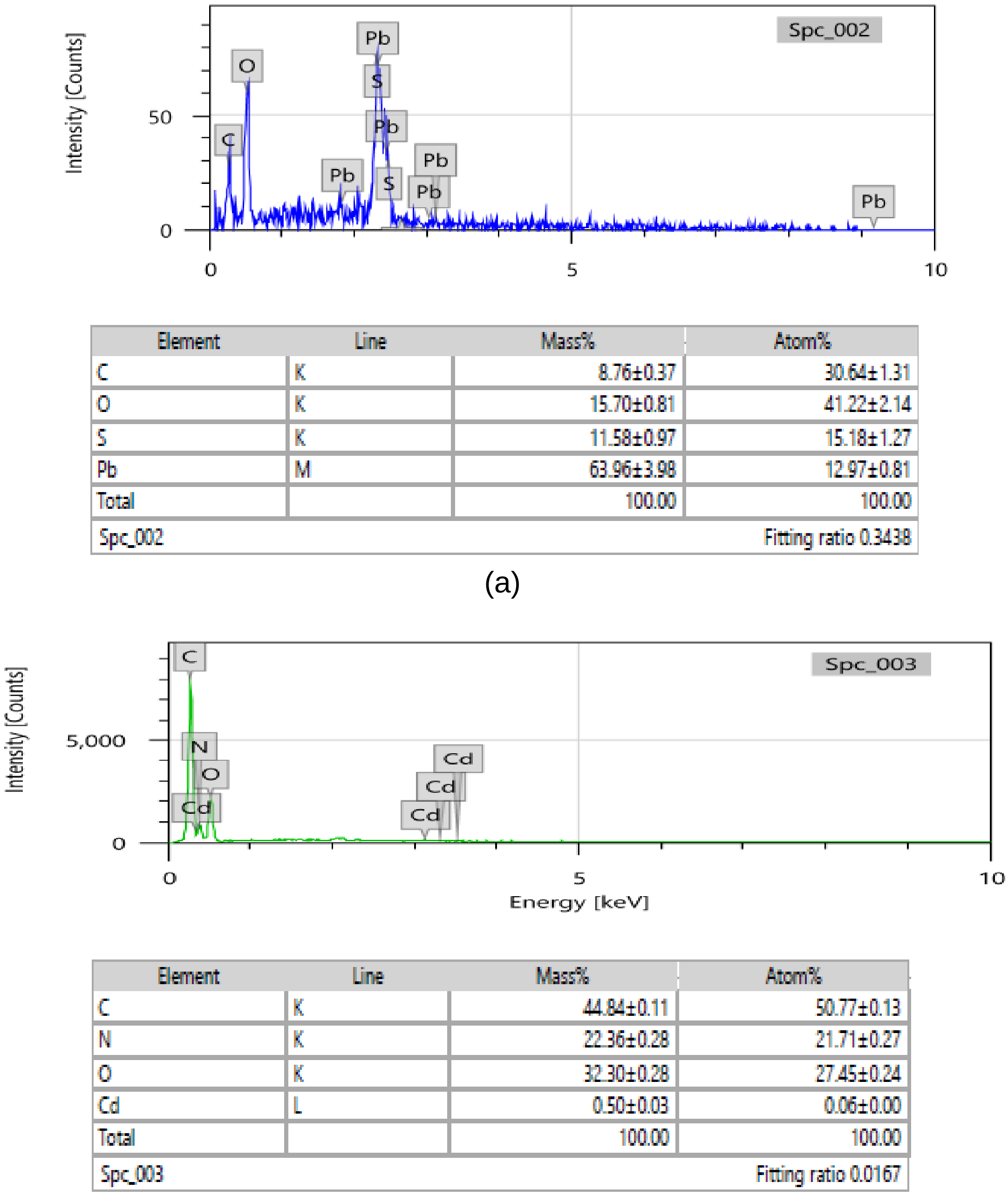

Element	Line	Mass%	Atom%
C	K	8.76±0.37	30.64±1.31
O	K	15.70±0.81	41.22±2.14
S	K	11.58±0.97	15.18±1.27
Pb	M	63.96±3.98	12.97±0.81
Total		100.00	100.00
Spc_002			Fitting ratio 0.3438

(a)

Element	Line	Mass%	Atom%
C	K	44.84±0.11	50.77±0.13
N	K	22.36±0.28	21.71±0.27
O	K	32.30±0.28	27.45±0.24
Cd	L	0.50±0.03	0.06±0.00
Total		100.00	100.00
Spc_003			Fitting ratio 0.0167

(b)

Figure 11. (a) EDS results of the $(CG\text{-}AM)_H$ Pb^{2+} after adsorption and (b) $(CG\text{-}AM)_H$ Cd^{2+} after adsorption

4. Conclusion

This study investigated the synthesis of $(CG\text{-}AM)_H$ for the removal of Pb^{2+} and Cd^{2+} removal from the stock solution of lead nitrate and cadmium sulfate by free radical polymerization. A maximum hydrogel yield of 4.527 was gained at the low level of hydration ratio, medium level of monomer amount and low level of crosslinking concentration. Hydrogel for Pb^{2+} removal of 86.985% was found at the medium level of hydration ratio and low level of monomer amount and crosslinking concentration but for Cd^{2+} removal, a percentage of 18.75% was found at the lower level of hydration ratio and a higher level of monomer amount and medium level of crosslinking concentration respectively. According to the FTIR results, it can be concluded that the major functional groups that collaborated in the complex formation Pb^{2+} and hydrogel were carboxylate (COO), –C=O (carbonyl), and –OH (hydroxyl) groups of carboxylic acid and NH_2 (amine) group of amino acid, C-O stretching of S-glycosidic bond of hydrogel and the presence of these compound were effective for removing of metal ion. From the XRD result, except $(CG\text{-}AM)_H$ Cd^{2+} amorphous nature of hygroscopic properties was seen in other prepared hydrogel. A crosslinked network structure with open pores was found in $(CG\text{-}AM)_H$ Pb^{2+} from the SEM result. Lead (Pb+) metal with the highest mass percentage of 63.96 on the $(CG\text{-}AM)_H$ Pb^{2+} sample surface was found from the EDS result. Therefore, the synthesis of hydrogel from CG polysaccharide (arabinogalactan) based monomer (acrylamide) can be used as an economical porous adsorbent for Pb^{2+}removal. For Cd $^{2+}$ removal, $(CG\text{-}AM)_H$ Cd $^{2+}$ was not effective because of the residue of monomer (AM) in the prepared hydrogel. It can be concluded that incomplete washing of monomer (AM) during the preparation of hydrogel can influence the adsorption of metal ions on the hydrogel surface and reduce removal efficiency.

Acknowledgements

The authors are thankful to the Department of National Laboratory at the Department of Research and Innovation (DRI), Myanmar Japan Development Technological Center (MJDTC) at Yangon Technological University (YTU) for being allowed to analyze this research work.

Declarations

Author contribution

Aye Thwe Thwe Soe: Conception of methodology, experimental design, writing the manuscript, reviewing and editing. May Myat Khine: Conceptualisation of experimental design, methodology, supervision, review and editing

Funding statement

We declare that we have received no specific financial support for this research from any individual or public group.

Competing interest

The authors declare no competing interests.

Ethical Clearance

This research does not involve human subjects.

References

ALSamman, M. T., & Sánchez, J. (2023). Adsorption of Copper and Arsenic from Water Using a Semi-Interpenetrating Polymer Network Based on Alginate and Chitosan. *Polymers*, *15*(9), 2192. https://doi.org/10.3390/polym15092192

Anamica, & Pande, P. P. (2017). Polymer Hydrogels and Their Applications. *International Journal of Materials Science*, *12*(1), 11–14. https://www.ripublication.com/ijoms17spl/ijomsv12n1spl_03.pdf

Barros, D. M. A., Edvan, R. L., Pessoa, J. P. M., do Nascimento, R. R., Camboim, L. F. R., Bezerra, L. R., de Araújo, M. J., de Sousa, H. R., & Silva-Filho, E. C. (2023). Hydrogel Based on Cashew Gum and Polyacrylamide as a Potential Water Supplier in Mombaça Grass Pastures: A Sustainable Alternative for Agriculture. *Sustainability*, *15*(23), 16423. https://doi.org/10.3390/su152316423

Bezerra, M. A., Santelli, R. E., Oliveira, E. P., Villar, L. S., & Escaleira, L. A. (2008). Response surface methodology (RSM) as a tool for optimization in analytical chemistry. *Talanta*, *76*(5), 965–977. https://doi.org/10.1016/j.talanta.2008.05.019

Choudhary, P. D., & Pawar, H. A. (2014). Recently Investigated Natural Gums and Mucilages as Pharmaceutical Excipients: An Overview. *Journal of Pharmaceutics*, *2014*, 1–9. https://doi.org/10.1155/2014/204849

Chowdhury, I. R., Chowdhury, S., Mazumder, M. A. J., & Al-Ahmed, A. (2022). Removal of lead ions (Pb2+) from water and wastewater: a review on the low-cost adsorbents. *Applied Water Science*, *12*(8), 185. https://doi.org/10.1007/s13201-022-01703-6

Darban, Z., Shahabuddin, S., Gaur, R., Ahmad, I., & Sridewi, N. (2022). Hydrogel-Based Adsorbent Material for the Effective Removal of Heavy Metals from Wastewater: A Comprehensive Review. *Gels*, *8*(5), 263. https://doi.org/10.3390/gels8050263

El Amri, A., Bensalah, J., Kadiri, L., Essaadaoui, Y., Lebkiri, I., Zarrouk, A., Rifi, E. H., & Lebkiri, A. (2022). Investigation of the cellulose reed plant as a potential adsorbent to remove Pb(II): equilibrium isotherms and thermodynamic studies. *DESALINATION AND WATER TREATMENT*, *262*, 137–151. https://doi.org/10.5004/dwt.2022.28564

Glycoside - Wikipedia. (n.d.). Retrieved May 19, 2024, from https://en.wikipedia.org/wiki/Glycoside

Kannan, N., & Seenivasan, R. K. (2006). Synthesis, characterization, and application of new low-cost ion exchangers. *Journal of Applied Polymer Science*, *101*(6), 4104–4113. https://doi.org/10.1002/app.23432

Kumar, A., Raizaday, A., Gopal, U. M., & Moin, A. (2014). Development of cashew gum and its derivatives for sustained released drug delivery system: By response surface methodology. *International Journal of Pharmacy and Pharmaceutical Sciences*, *6*(10), 476–687.

Ma, Y., & Johnson, K. (2023). Arabinogalactan proteins – Multifunctional glycoproteins of the plant cell wall. *The Cell Surface*, *9*, 100102. https://doi.org/10.1016/j.tcsw.2023.100102

Mahmoud, G. A., & Mohamed, S. F. (2012). Removal of lead ions from aqueous solution using (sodium alginate/itaconic acid) hydrogel prepared by gamma radiation. *Australian Journal of Basic and Applied Sciences*, *6*(6).

Mandal, B., & Ray, S. K. (2014). Swelling, diffusion, network parameters and adsorption properties of IPN hydrogel of chitosan and acrylic copolymer. *Materials Science and Engineering: C*, *44*, 132–143. https://doi.org/10.1016/j.msec.2014.08.021

Mansoorian, H. J., Mahvi, A. H., & Jafari, A. J. (2014). Removal of lead and zinc from battery industry wastewater using electrocoagulation process: Influence of direct and alternating current by using iron and stainless steel rod electrodes.

Separation and Purification Technology, *135*, 165–175. https://doi.org/10.1016/j.seppur.2014.08.012

Mehdipour, S., Vatanpour, V., & Kariminia, H.-R. (2015). Influence of ion interaction on lead removal by a polyamide nanofiltration membrane. *Desalination*, *362*, 84–92. https://doi.org/10.1016/j.desal.2015.01.030

Ologunagba, M., Azubuike, C., Olanrewaju, S., Jain, S., Thanki, K., Suresh, S., & Furtado, S. (2017). Extraction and Characterization of the Gum Exudate of Anacardium occidentale for its potential as an Excipient in Drug Delivery Systems. *Tropical Journal of Natural Product Reseach*, *1*(2), 76–83. https://doi.org/10.26538/tjnpr/v1i2.6

Olorunsola, E. O., Bhatia, P. G., Tytler, B. A., & Adikwu, M. U. (2016). Thermochemical Properties of Hydrophilic Polymers from Cashew and Khaya Exudates and Their Implications on Drug Delivery. *Journal of Drug Delivery*, *2016*, 1–7. https://doi.org/10.1155/2016/7496585

Sharma, G., Kumar, A., Ghfar, A. A., García-Peñas, A., Naushad, Mu., & Stadler, F. J. (2021). Fabrication and Characterization of Xanthan Gum-cl-poly(acrylamide-co-alginic acid) Hydrogel for Adsorption of Cadmium Ions from Aqueous Medium. *Gels*, *8*(1), 23. https://doi.org/10.3390/gels8010023

Soro, L. P., Kouakou, M. D., & Soumaila, D. (2017). Application of Statistical Experiment design for pre-optimization of crude gum from cashew tree (Anacardium occidentale L.) exudates by aqueous extraction. *International Journal of Agriculture Innovations and Research*, *5*(6), 944–949. https://www.ijair.org/administrator/components/com_jresearch/files/publications/IJAIR_2344_FINAL.pdf

Soro, L. P., Dje, K. M., & Dabonné, S. (2018). Optimization of Crude Gum Extraction from Cashew Tree (Anacardium occidentale L.) Exudates by Response Surface Methodology Using Box-Behnken Design. *International Research Journal of Engineering and Technology*, *5*(9), 813–822. https://www.irjet.net/archives/V5/i9/IRJET-V5I9147.pdf

Sousa, R. H., Lima, I. S., Neris, L. M. L., Silva, A. S., Santos Nascimento, A. M. S., Araújo, F. P., Ratke, R. F., Silva, D. A., Osajima, J. A., Bezerra, L. R., & Silva-Filho, E. C. (2021). Superabsorbent Hydrogels Based to Polyacrylamide/Cashew Tree Gum for the Controlled Release of Water and Plant Nutrients. *Molecules*, *26*(9), 1–19. https://doi.org/10.3390/molecules26092680

Trivedi, M. K., Patil, S., Mishra, R., & Jana, S. (2015). Characterization of Thermal and Physical properties of Biofield Treated Acrylamide and 2-Chloroacetamide. *Organic Chemistry: Current Research*, *4*(3), 1–6. https://doi.org/10.4172/2161-0401.1000143

Vergili, I., Gönder, Z. B., Kaya, Y., Gürdağ, G., & Çavuş, S. (2017). Lead removal from battery wastewater using synthesized poly(ethyleneglycol dimethacrylate-methacrylic acid) gel bead and poly (methacrylic acid) hydrogel. *Polymer Bulletin*, *74*(7), 2605–2624. https://doi.org/10.1007/s00289-016-1855-4

WHO. (2011). *Acrylamide in drinking-water*. Water Sanitation Health, WHO/SDE/WSH/03.04/71.

Zhao, L., & Mitomo, H. (2008). Adsorption of heavy metal ions from aqueous solution onto chitosan entrapped CM-cellulose hydrogels synthesized by irradiation. *Journal of Applied Polymer Science*, *110*(3), 1388–1395. https://doi.org/10.1002/app.28718